

Title	Piezoelectric inkjet coating of injection moulded, reservoir-tipped microneedle arrays for transdermal delivery
Authors	O'Mahony, Conor;Bocchino, Andrea;Haslinger, Michael J.;Brandstätter, Stefan;Außerhuber, Helene;Schossleitner, Klaudia;Clover, Anthony J. P.;Fechtig, Daniel
Publication date	2019-06-04
Original Citation	O'Mahony, C., Bocchino, A., Haslinger, M. J., Brandstätter, S., Außerhuber, H., Schossleitner, K., Clover, A. J. P. and Fechtig, D. (2019) 'Piezoelectric inkjet coating of injection moulded, reservoir-tipped microneedle arrays for transdermal delivery', Journal of Micromechanics and Microengineering, 29 (8), 085004 (8 pp). doi: 10.1088/1361-6439/ab222b
Type of publication	Article (peer-reviewed)
Link to publisher's version	https://iopscience.iop.org/article/10.1088/1361-6439/ab222b/meta - 10.1088/1361-6439/ab222b
Rights	© 2019 IOP Publishing Ltd. This is an author-created, uncopyedited version of an article accepted for publication in Journal of Micromechanics and Microengineering. The publisher is not responsible for any errors or omissions in this version of the manuscript or any version derived from it. The Version of Record is available online at https://doi.org/10.1088/1361-6439/ab222b . - https://creativecommons.org/licences/by-nc-nd/3.0
Download date	2025-04-24 09:46:13
Item downloaded from	https://hdl.handle.net/10468/8401



UCC

University College Cork, Ireland
Coláiste na hOllscoile Corcaigh

ACCEPTED MANUSCRIPT

Piezoelectric inkjet coating of injection moulded, reservoir-tipped microneedle arrays for transdermal delivery

To cite this article before publication: Conor O'Mahony *et al* 2019 *J. Micromech. Microeng.* in press <https://doi.org/10.1088/1361-6439/ab222b>

Manuscript version: Accepted Manuscript

Accepted Manuscript is “the version of the article accepted for publication including all changes made as a result of the peer review process, and which may also include the addition to the article by IOP Publishing of a header, an article ID, a cover sheet and/or an ‘Accepted Manuscript’ watermark, but excluding any other editing, typesetting or other changes made by IOP Publishing and/or its licensors”

This Accepted Manuscript is © 2019 IOP Publishing Ltd.

During the embargo period (the 12 month period from the publication of the Version of Record of this article), the Accepted Manuscript is fully protected by copyright and cannot be reused or reposted elsewhere.

As the Version of Record of this article is going to be / has been published on a subscription basis, this Accepted Manuscript is available for reuse under a CC BY-NC-ND 3.0 licence after the 12 month embargo period.

After the embargo period, everyone is permitted to use copy and redistribute this article for non-commercial purposes only, provided that they adhere to all the terms of the licence <https://creativecommons.org/licenses/by-nc-nd/3.0>

Although reasonable endeavours have been taken to obtain all necessary permissions from third parties to include their copyrighted content within this article, their full citation and copyright line may not be present in this Accepted Manuscript version. Before using any content from this article, please refer to the Version of Record on IOPscience once published for full citation and copyright details, as permissions will likely be required. All third party content is fully copyright protected, unless specifically stated otherwise in the figure caption in the Version of Record.

View the [article online](#) for updates and enhancements.

Piezoelectric Inkjet Coating of Injection Moulded, Reservoir-Tipped Microneedle Arrays for Transdermal Delivery

Conor O'Mahony^{1,*}, Andrea Bocchino¹, Michael J. Haslinger², S. Brandstätter³, Helene Außerhuber², Klaudia Schossleitner⁴, A. James P. Clover⁵, and Daniel Fechtig²

¹Tyndall National Institute, University College Cork, Cork, Ireland.

²PROFACTOR GmbH, Steyr-Gleink, Austria.

³STRATEC Consumables GmbH, Anif, Austria.

⁴Skin and Endothelium Research Division, Department of Dermatology, Medical University Vienna, Vienna, Austria

⁵Department of Plastic and Reconstructive Surgery, Cork University Hospital, Cork, Ireland.

Email: conor.omahony@tyndall.ie

Abstract. Coated microneedles have significant potential for use in transdermal delivery applications. In this paper, we describe the fabrication of microneedle master templates using microstereolithography techniques and subsequently use a commercial injection moulding process to replicate these microneedles in biocompatible cyclic olefin polymer (COP) materials. Notably, the 475 μm -tall needle designs feature a shallow pit or reservoir at the tip, thereby providing both a target and holder for incoming droplets that are deposited using a piezoelectric inkjet printer. Using this design, no tilting or rotation of the needle array is required during the filling process. In the preliminary tests reported here, the reservoir is filled with a FITC-labelled dye that acts as a model drug, and *ex-vivo* skin tests are used to verify skin penetration, the transfer of this model drug to the skin and to measure the reliability of the needles themselves. To our knowledge, this is the first time that such an inkjet-filled, reservoir-tipped microneedle has been demonstrated.

Keywords - Microneedles, injection moulding, piezoelectric inkjet dispensing, bioMEMS, transdermal drug delivery, microstereolithography

Submitted to *Journal Of Micromechanics and Microengineering*, 14-01-19

Revised 01-05-19

1 Introduction

Patch-based transdermal drug delivery is highly attractive due to its needle-free nature and potential for self-administration, with corresponding benefits in increased patient compliance, reduced clinical time, elimination of needle-stick injuries and sharps waste. However, the outermost layer of the skin poses a formidable barrier to the transdermal delivery of drugs and vaccines. Despite being relatively thin (typically 10-20 μ m thick), the *stratum corneum* prevents the passage of all but a small number of low molecular weight drugs, currently estimated at fewer than 20 products [1-3]. However, this specialized and constantly renewing layer of cornified and keratin-rich cell bodies is not the only hurdle to overcome. The skin barrier is further fortified by a high number of cell-cell junctions in the epidermal layers beneath [4]. To efficiently deliver drugs across these multiple barriers in the epidermis of mammalian skin new transdermal drug delivery technologies are needed.

Microneedle technologies have been proposed as a potential solution to this issue. Consisting of short, sharp structures generally measuring less than 1 mm in length and provided in arrays of anything up to several thousand per square centimetre, microneedle patches can be used to penetrate the *stratum corneum* and deliver drugs or vaccines to the viable epidermis immediately below in a painless and minimally invasive manner [5, 6].

These arrays can be deployed in four primary delivery mechanisms. Firstly, simple solid microneedles can be used to painlessly perforate the skin before the subsequent application of a topical formulation or patch [7]. Secondly, drugs and vaccines can be infused in small volumes and at low flowrates through hollow microneedles in much the same manner as with conventional hypodermic needles [8]. Thirdly, a number of techniques such as brushing, dipping, inkjet printing or spraying can be used to coat microneedles with a formulation that is dried and later dissolved in the skin [9]. Lastly, dissolvable microneedles (DMNs) are moulded from a biodegradable polymer into which a drug or vaccine is mixed and which dissolves once in contact with the moist epidermal layers beneath the *stratum corneum* [10].

1.1 Low-cost transdermal drug delivery (TDD) device fabrication

Microneedles have traditionally been fabricated using techniques borrowed from the semiconductor industry, such as photolithography, thin-film deposition, wet and dry etching, and wafer dicing [11, 12]. Although precise and in some cases capable of producing complex and ultrasharp devices that integrate additional functionality such as fluidics and electronics, semiconductor-based processing is expensive, often slow, and tends to use materials that may not be accepted as standard in the medical devices industry. Therefore, there is growing interest in the low-cost, rapid fabrication of transdermal

1
2
3 drug delivery systems (TDDS), using a combination of one or more techniques for fabrication,
4 replication and/or functionalization [13]. Micromoulding has attracted wide interest for low-cost
5 microneedle fabrication, using both solid [14] and biodegradable [15] materials. In particular,
6 biodegradable microneedles have the advantage that the drug or vaccine of interest may be mixed
7 with the structural material. This provides a single-step fabrication process and a low-cost delivery
8 route with the potential for relatively high dose loading [16], and significant progress is being made in
9 addressing issues such as polymer processing temperatures, biomechanical strength and long-term
10 stability during storage [17]. Alternative processes that may provide low-temperature fabrication, such
11 as droplet air blowing [18] and drawing lithography [19], are also emerging as candidates for low-cost
12 needle manufacture.

13
14 Among more commercially established technologies, injection moulding is commonly used for the
15 manufacture of biomedical components [20, 21], and has been shown to be capable of replicating the
16 small features and sharp tips usually associated with microneedles, in low cost, high-throughput
17 facilities. 3M Corporation have demonstrated transdermal drug delivery using both solid [22-24] and
18 hollow [25] injection moulded microneedles, fabricated from medical-grade, liquid crystalline
19 polymer materials under their Microstructured Transdermal System (MTS) brand. Others have used
20 injection moulding techniques to create microneedles in materials such as polycarbonate,
21 polyethylene terephthalate (PET), cyclic olefin copolymer (COC), and polyoxymethylene [26-29].

22
23 3D printing approaches such as two-photon polymerization (2PP), microstereolithography (μ SL) or
24 digital light processing (DLP) are also emerging as a new way of making microneedles, and can now
25 achieve very precise geometries [30]. Ultra-sharp polymer microneedles specifically designed to
26 perforate the round window membrane (RWM) of the inner ear with a view to precisely delivering
27 therapeutics across that membrane were fabricated using 2PP [31], achieving a tip radius of 500 nm.
28 2PP was also employed to fabricate 630 nm-diameter microneedles for use in single cell analysis from
29 a drop cast resist material [32], while μ SL was used to develop 700 μ m tall biodegradable
30 microneedles for chemotherapeutic drug delivery [33]. 3D printing has also been used to fabricate a
31 curved microneedle array for treatment of trigger finger, and to subsequently deliver diclofenac gel
32 using the 'poke and patch' approach [34].

33
34 These low-cost 3D printing approaches can be merged with non-contact coating techniques,
35 particularly piezoelectric inkjet deposition [35, 36], to form fully functional transdermal drug delivery
36 patches. The team at University of North Carolina and North Carolina State University, have
37 combined μ SL and elastomeric vacuum casting to create microneedles from Gantrez polymers, which
38 were then coated with various formulations using piezoelectric printing [37-39]. Later, that group
39 used a combination of injection moulding, drawing lithography and piezoelectric printing to
40 demonstrate poly(glycolic) acid microneedles that were coated with itraconazole and voriconazole
41 formulations [40, 41]. In all cases, deposition was facilitated by carefully arranging the needles so that

1
2
3 a flat face of the needle was positioned at 90° to the incoming droplet path, and in [41], loading was
4 maximised by rotating the needle midway through the process in order to coat both sides. In [42], μ SL
5 printing and inkjet disposition were combined for applications in insulin delivery.
6
7

8
9 Clearly, in studies performed to date, multiple coating steps or careful positioning of the microneedle
10 array substrate is required in order to obtain sufficiently high dose loading. An alternative method of
11 increasing dose loading, without using substrate orientation or multiple deposition passes, could be by
12 modifying the structure of the microneedle tip itself to receive and to hold larger volumes of
13 formulation. In this paper, we therefore describe the fabrication of microneedle master templates
14 using μ SL techniques and show that it is possible to use a commercial injection moulding process to
15 replicate these microneedles in cyclic olefin polymers (COPs), with shape and sharpness approaching
16 that of the original master template. Notably, the microneedles have been designed to incorporate a
17 shallow pit or reservoir at the tip, thereby providing both a target and holder for incoming droplets
18 that are deposited using a piezoelectric inkjet printer. This reservoir retains the formulation close to
19 the tip, and also has the potential to increase loading capacity. In the preliminary tests reported here,
20 the reservoir is filled with a FITC-labelled dye that acts as a model drug, and *ex-vivo* skin tests are
21 used to verify the transfer of this model drug to the skin. In addition, we measure the reliability of the
22 needles themselves. To our knowledge, this is the first time that such a reservoir-tipped microneedle
23 has been demonstrated.
24
25
26
27
28
29
30
31
32

33 **2 Experimental Details**

34 *2.1 Microneedle master – design and fabrication*

35
36
37
38
39 Microneedle master templates were produced using microstereolithography (μ SL), i.e the spatially
40 controlled solidification of a liquid resin by direct ultraviolet photo-polymerization in a series of
41 layers. The microneedles were designed as 475 μ m tall, cone-like structures with a sidewall angle of
42 73°, at a pitch of 1.4 mm, and incorporating a 180 μ m deep reservoir (volume approximately 59 pL)
43 near the tip, figure 1. This bevel-like, offset design positions the drug cargo close to the tip, whilst
44 retaining the tip itself for better skin penetration and needle reliability.
45
46
47
48

49
50
51
52
53
54
55
56
57
58
59
60
61
62
63
64
65
66
67
68
69
70
71
72
73
74
75
76
77
78
79
80
81
82
83
84
85
86
87
88
89
90
91
92
93
94
95
96
97
98
99
100
101
102
103
104
105
106
107
108
109
110
111
112
113
114
115
116
117
118
119
120
121
122
123
124
125
126
127
128
129
130
131
132
133
134
135
136
137
138
139
140
141
142
143
144
145
146
147
148
149
150
151
152
153
154
155
156
157
158
159
160
161
162
163
164
165
166
167
168
169
170
171
172
173
174
175
176
177
178
179
180
181
182
183
184
185
186
187
188
189
190
191
192
193
194
195
196
197
198
199
200
201
202
203
204
205
206
207
208
209
210
211
212
213
214
215
216
217
218
219
220
221
222
223
224
225
226
227
228
229
230
231
232
233
234
235
236
237
238
239
240
241
242
243
244
245
246
247
248
249
250
251
252
253
254
255
256
257
258
259
260
261
262
263
264
265
266
267
268
269
270
271
272
273
274
275
276
277
278
279
280
281
282
283
284
285
286
287
288
289
290
291
292
293
294
295
296
297
298
299
300
301
302
303
304
305
306
307
308
309
310
311
312
313
314
315
316
317
318
319
320
321
322
323
324
325
326
327
328
329
330
331
332
333
334
335
336
337
338
339
340
341
342
343
344
345
346
347
348
349
350
351
352
353
354
355
356
357
358
359
360
361
362
363
364
365
366
367
368
369
370
371
372
373
374
375
376
377
378
379
380
381
382
383
384
385
386
387
388
389
390
391
392
393
394
395
396
397
398
399
400
401
402
403
404
405
406
407
408
409
410
411
412
413
414
415
416
417
418
419
420
421
422
423
424
425
426
427
428
429
430
431
432
433
434
435
436
437
438
439
440
441
442
443
444
445
446
447
448
449
450
451
452
453
454
455
456
457
458
459
460
461
462
463
464
465
466
467
468
469
470
471
472
473
474
475
476
477
478
479
480
481
482
483
484
485
486
487
488
489
490
491
492
493
494
495
496
497
498
499
500
501
502
503
504
505
506
507
508
509
510
511
512
513
514
515
516
517
518
519
520
521
522
523
524
525
526
527
528
529
530
531
532
533
534
535
536
537
538
539
540
541
542
543
544
545
546
547
548
549
550
551
552
553
554
555
556
557
558
559
560
561
562
563
564
565
566
567
568
569
570
571
572
573
574
575
576
577
578
579
580
581
582
583
584
585
586
587
588
589
590
591
592
593
594
595
596
597
598
599
600
601
602
603
604
605
606
607
608
609
610
611
612
613
614
615
616
617
618
619
620
621
622
623
624
625
626
627
628
629
630
631
632
633
634
635
636
637
638
639
640
641
642
643
644
645
646
647
648
649
650
651
652
653
654
655
656
657
658
659
660
661
662
663
664
665
666
667
668
669
670
671
672
673
674
675
676
677
678
679
680
681
682
683
684
685
686
687
688
689
690
691
692
693
694
695
696
697
698
699
700
701
702
703
704
705
706
707
708
709
710
711
712
713
714
715
716
717
718
719
720
721
722
723
724
725
726
727
728
729
730
731
732
733
734
735
736
737
738
739
740
741
742
743
744
745
746
747
748
749
750
751
752
753
754
755
756
757
758
759
760
761
762
763
764
765
766
767
768
769
770
771
772
773
774
775
776
777
778
779
780
781
782
783
784
785
786
787
788
789
790
791
792
793
794
795
796
797
798
799
800
801
802
803
804
805
806
807
808
809
810
811
812
813
814
815
816
817
818
819
820
821
822
823
824
825
826
827
828
829
830
831
832
833
834
835
836
837
838
839
840
841
842
843
844
845
846
847
848
849
850
851
852
853
854
855
856
857
858
859
860
861
862
863
864
865
866
867
868
869
870
871
872
873
874
875
876
877
878
879
880
881
882
883
884
885
886
887
888
889
890
891
892
893
894
895
896
897
898
899
900
901
902
903
904
905
906
907
908
909
910
911
912
913
914
915
916
917
918
919
920
921
922
923
924
925
926
927
928
929
930
931
932
933
934
935
936
937
938
939
940
941
942
943
944
945
946
947
948
949
950
951
952
953
954
955
956
957
958
959
960
961
962
963
964
965
966
967
968
969
970
971
972
973
974
975
976
977
978
979
980
981
982
983
984
985
986
987
988
989
990
991
992
993
994
995
996
997
998
999
1000

Needles were printed using a custom-built μ SLA system using a 375 nm UV-laser diode and a scanning galvanometer mirror to solidify a UV-curing adhesive (07A22X-8, Sony CID Corp., Tokyo). First, a square base for the arrays was printed using 4 x 100 μ m thick layers. Next, 5 μ m thick layers were used to create the lower body of the needle, while the layer thickness was reduced to 2 μ m for the last 15 layers. This smaller step height results in increased accuracy and tip sharpness. Arrays of 5 x 5 needles were produced, and the printing time for one array was roughly 5 hours, depending on the final resolution and chosen layer thickness.

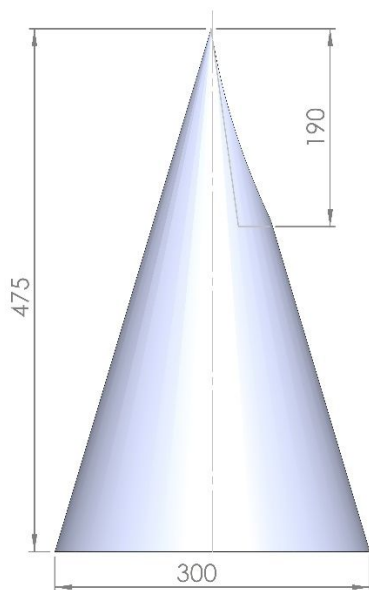


Figure 1. CAD drawing of the microneedle master design.

2.2 Injection Moulding

Using these templates, arrays of sharp polymer microneedle structures were then manufactured at STRATEC Consumables GmbH (Anif, Austria), using a proprietary replication process based on their former CD/DVD production equipment. This involved mounting a customized insert on an existing CD mould, and using an isothermal injection moulding process without compression. A Sumitomo Disc 40E Disc Molding Subsystem (Sumitomo SHI Demag Plastics Machinery North America, Inc., OH, USA) was used for moulding; the mould temperature was 80°C and the clamping pressure set at 25 tons, figure 2. The material was Zeonor 1020R cyclic olefin polymer (Zeon Europe GmbH, Dusseldorf, Germany), which we have already shown to be biocompatible according to ISO 10993-5 and USP 87 standards [43], and the process resulted in easy de-moulding as well as sharp needle tips. A milling procedure was then used to partially isolate each electrode from the frame, leaving the array lightly tethered on two thin supports for subsequent easy removal.



Figure 2. Sumitomo Disc 40E Disc Moulding Subsystem [44].

2.3 Piezoelectric dispensing

The injection moulded needles were then filled using a Dimatix DMP 2800 drop-on-demand inkjet printer (FujiFilm Dimatix, Santa Clara, CA). An actuation pulse of amplitude 15 V and duration of 11.5 μ s, and a maximum jetting frequency of 5000 Hz was used. Nominal drop volume was 10pL and the escape velocity of the droplets was between 2-8 m/s.

The ink was a mixture of 5 wt % fluorescein isothiocyanate (FITC) dye for imaging purposes, 22 wt % water and a 73 wt % mixture of volatile solvents. The dry mass of one drop (FITC) was 0.536 ng per drop. The ink temperature was set to 50 °C, and the printbed was heated to 30 °C. Ambient laboratory conditions (20 °C and relative humidity of 50 %) prevailed. Loaded needles were then dried at 100 °C for 30 minutes.

For these initial tests and to aid with subsequent visualisation of the dye transfer to skin, just one column of each array (i.e 5 x 1 needles) was loaded. Initially the array was aligned with one axis of the printer, and the coordinates of the first needle in the target row were selected using the printhead camera and Dimatix internal software. Subsequent needles were coated by moving the nozzle along the row, in steps equal to the microneedle pitch, starting from the location of this first needle. A variety of deposition settings and skin insertion times were used as specified in Table 1 below.

2.4 Skin preparation and array applications

Following protocols approved by the Clinical Research Ethics Committee of the Cork Teaching Hospitals (CREC), human skin was excised following plastic surgical operations and stored at -80 °C until needed. It was then defrosted, trimmed of excess fat, cut into squares of approximately 3 cm x 3 cm, and mounted on an artificial tissue substrate (Wound Closure Pad, Limbs & Things, Bristol, UK) to mimic the mechanical properties of underlying tissue.

Spring-loaded applicators are often used to apply microneedle devices to the skin in a consistent manner [45]. In this case, a custom-built applicator was used to ensure repeatable and reliable skin penetration. This applicator uses a spring constant of 274 N/m, and generated impact energy of (0.4 +/- 0.01) J/cm².

Methylene blue staining is a technique routinely used to assess microneedle penetration [46], and was also used here to confirm skin breach. During this procedure, uncoated arrays (i.e. with empty tip reservoirs) were applied to the skin with the applicator and left in place for 20 minutes. After removal, the impact area was stained with a 1% solution (w/vol) of methylene blue (Sigma-Aldrich, Dublin, Ireland) for 90 minutes. Excess dye was removed with tissue, the skin was cleaned with water and 70% ethanol, before being tape stripped ten times (9040 Paper Tape, 3M Corp., St Paul, MN) in order to ensure than any remaining dye was present under the stratum corneum and not on its surface.

To test the fluorescent dye-loaded microneedle arrays, the applicator maintained a force of (5.90 +/- 0.54) N on the needle array for a specific time after impact. Six arrays were tested at varying insertion times, see Table 1.

Array Number	# drops	Nominal Volume (pL)	Total Dry Mass (ng)	Insertion Time (min)
1	2	20	1,072	10
2	4	40	2,144	10
3	4	40	2,144	5
4	6	60	3,216	5
5	6	60	3,216	1
6	8	80	4,288	1

Table 1. Needle loading parameters and skin insertion times for each sample type.

2.5 Inspection and classification

Optical microscope images of the methylene blue-stained impact area after insertion and skin washing/stripping were recorded using a digital camera. A thorough inspection of the fluorescent dye-loaded needles was also performed. Each of the 6 injection moulded arrays featured 21 needles – a total of 126 needles. Of these, one column (five needles) on each array was filled. Each needle, whether filled or not, was individually inspected both before and after skin insertion, from a variety of angles and orientations, using microscopes including stereozoom (SZX12, Olympus Corp., Tokyo, Japan), digital (VHX-200, Keyence Ltd., Milton Keynes, UK) and fluorescent (Olympus BX51). The purpose of this exercise was to visually confirm delivery of the dye and to assess any damage that occurred during the insertion process.

Following application to *ex-vivo* tissue as outlined above, fluorescent microscopy was used to examine the transfer of material from filled needles to skin. Pictures of the surface of the skin were taken with the fluorescent microscope at exposure times (ETs) of 50 ms, 100 ms and 200 ms.

Finally, the skin samples were cut using a scalpel along the line of the holes left by the loaded needles. Images of the cross section of the skin were taken with the fluorescent microscope to assess the diffusion of the dye underneath the stratum corneum.

In order to quantify the intensity of the fluorescence as a function of array insertion time, an image analysis was performed using the software ImageJ [47]. A region of interest (ROI) was defined by firstly selecting an initial pixel at the boundary of the fluorescent area, and then using the software's 'Wand' tool to identify a contiguous area based on the condition that all the boundary pixel values

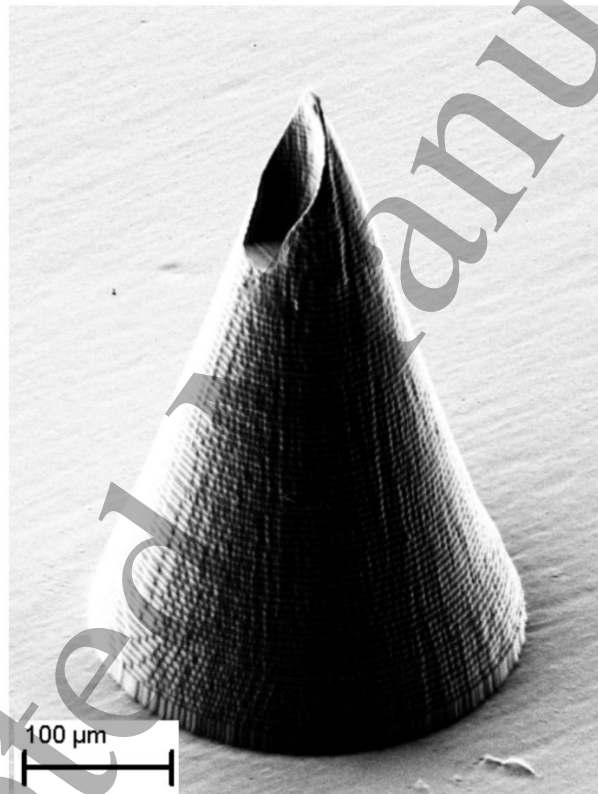
1
2
3 must be in the range *initial pixel value* \pm *tolerance*, where the tolerance value was set to 22 and kept
4 constant for each image analysis.
5

6
7 To remove the influence of the background signal, the mean intensity per pixel of the region outside
8 of the ROI was calculated for each image, and subtracted from each pixel within the ROI. The total
9 intensity was calculated by summing this net fluorescence per pixel over all pixels within the ROI.
10
11

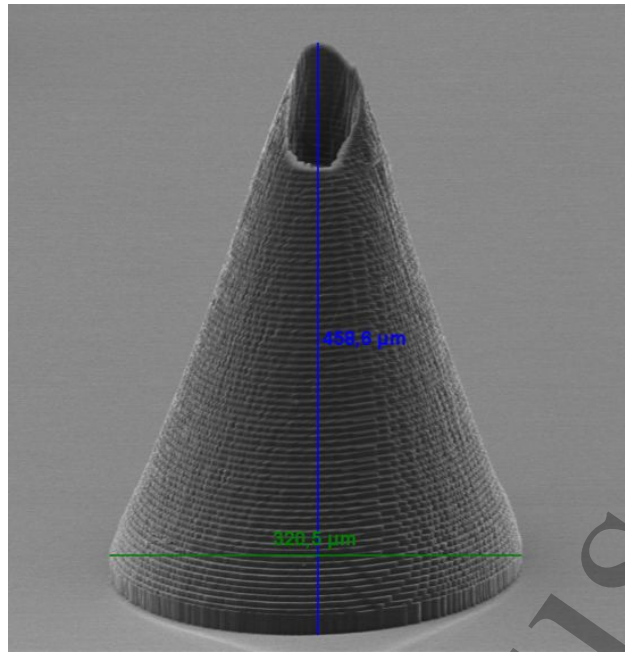
12 **3 Results and Discussion**

13 **3.1 Microneedle fabrication using μ SL and injection moulding**

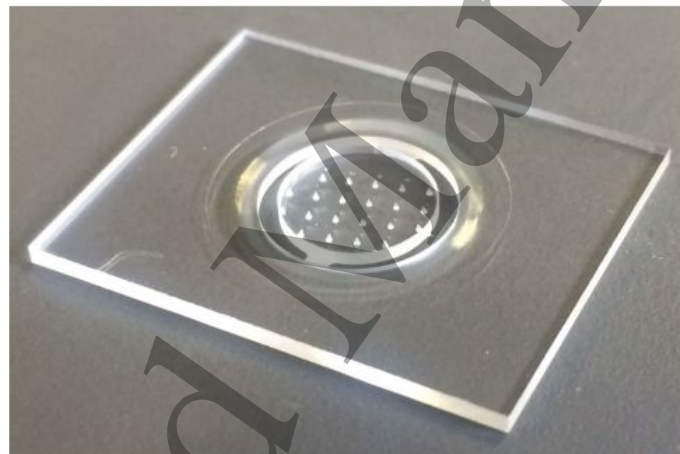
14
15
16 Images of the μ SL master structure and injection-moulded needle array are illustrated in figure 3.
17
18 Note the milled slot and tethers linking the array to the support frame.
19
20
21



48 (a)
49
50
51
52
53
54
55
56
57
58
59
60



(b)



(c)

Figure 3. (a) SEM image of μ SL master structure, (b) SEM of injection moulded microneedle, and (c) injection moulded array prior to removal from support frame.

3.2 Filling of needle reservoirs

Background fluorescence from the epoxy material itself prevented a thorough analysis of the polymer microneedle coating using fluorescence microscopy, and so droplet location and consistency was assessed using optical microscopy, figure 4. In general all of the incoming material was positioned in the reservoir and little or no splashing was observed on or around the needle.



Figure 4. Left: example of reservoir-tipped microneedles after the filling procedure. Right: Top-down perspective of filled microneedles.

3.3 Skin Penetration and Delivery

Penetration markings remaining after the staining procedure described in Section 2.4 are shown in figure 5.

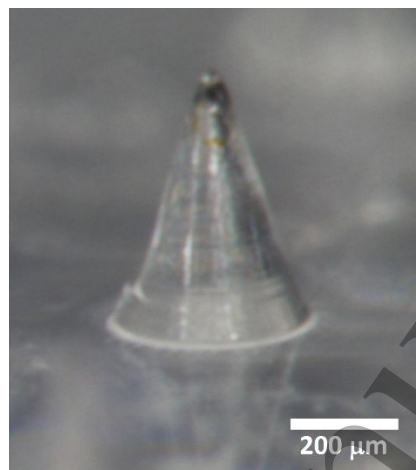


Figure 5. Ex-vivo skin sample stained with methylene blue dye following microneedle array insertion. The needle pitch is 1.4 mm.

Methylene blue is hydrophilic with a low molecular weight, and the intact, hydrophobic stratum corneum cannot take up the stain. Once the stratum corneum barrier is disrupted, the dye diffuses through the newly created pores to the underlying epidermis, where it binds to the tissue due to its high affinity for proteins. Therefore, the presence of blue markings after microneedle application is generally regarded as definitive proof of successful insertion. Note that 19 marks are present, while

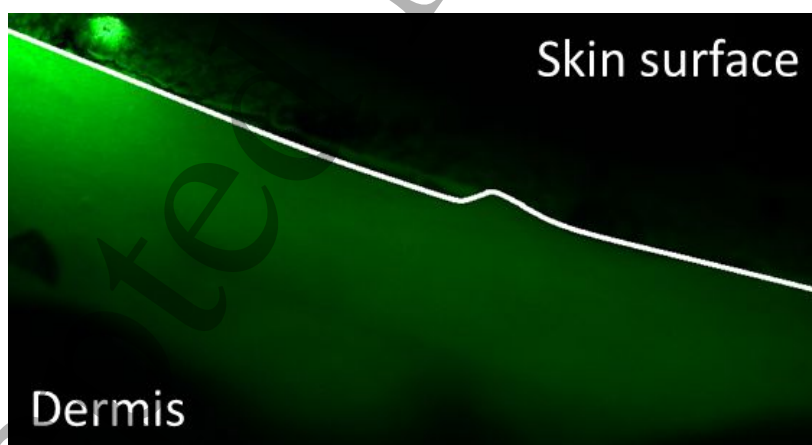
1
2
3 there are 21 needles on the array, and a closer inspection revealed that two needles on the right-hand
4 side of the array were damaged during handling, resulting in no penetration at these locations.

5
6 To establish if the fluorescent dye was delivered inside the skin, analysis of both the microneedle
7 arrays and skin samples was performed as outlined in Section 2.5. Figure 6 illustrates the needle
8 already shown in figure 4 after skin insertion for ten minutes.
9



28 *Figure 6. Microneedle of figure 3 (left) shown after skin insertion.*

29
30 The dye almost completely disappeared from the tip of the microneedle, indicating that it was
31 transferred to the skin. Further evidence of transdermal delivery is evident from the fluorescent photos
32 of the skin samples. As shown in figures 7 and 8, the points where the skin was pierced by the needles
33 are clearly visible and the fluorescent dye has diffused beneath the stratum corneum.
34
35
36



51
52 *Figure 7. Cross-section of skin sample. The point of needle insertion and diffusion of dye beneath the*
53 *surface is clearly visible.*

54
55 To quantify the dye delivery process as outlined in Section 2.5, the background contribution was
56 removed and the value of the fluorescence recalculated for the entire row of dye-loaded needles,
57 figure 8. Exposure time for all of this analysis was 50 ms (as longer exposures tended to exhibit
58
59
60

saturation) and the resultant intensity data is shown in figure 9. Two independent variables are present, i.e. droplet quantity and skin insertion time. In general, the results are as expected, i.e. increasing either the number of droplets or the skin insertion time results in an increase in fluorescent intensity.

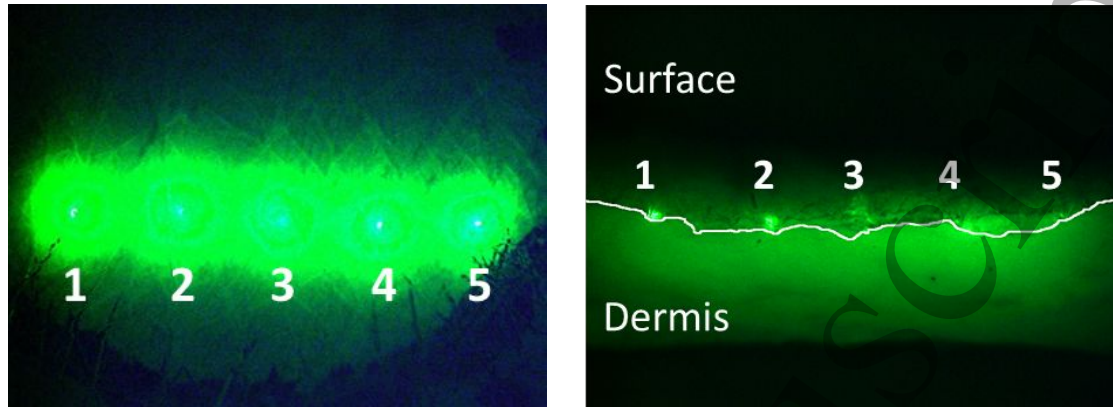


Figure 8. Delivery to skin. Left: En-face image. Right: cross-section of the same skin sample; the boundary between skin surface and underlying tissue is marked. Images taken after ten minutes insertion at 50 ms exposure time. The needle pitch is 1.4 mm.

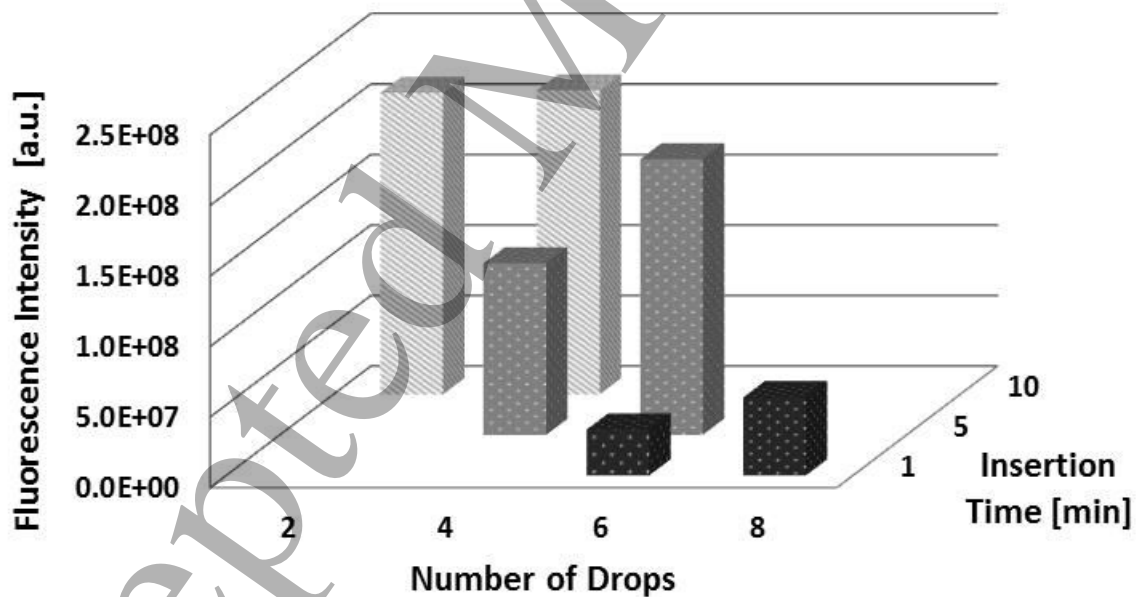


Figure 9. Fluorescence intensity as a function of skin insertion time and needle loading.

The only exception to this trend is for ten-minute insertion times, where the fluorescence intensities are much higher than for one- or five-minute insertion times, but do not vary significantly as a

1
2
3 function of loading volume. This may be caused by the skin becoming saturated after that period,
4 meaning that additional dye delivery does not alter the fluorescence readings.
5

6
7 This is the first demonstration of an injection-moulded, reservoir-tipped microneedle. However, this
8 preliminary proof-of-concept work is limited in scope and additional tests of larger sample sets are
9 required in order to draw definitive statistical conclusions. Secondly, while useful for initial device
10 validation during process development, this fluorescence method is somewhat limited due to its
11 projection of a three-dimensional diffusion pattern onto a two-dimensional image. Future
12 development will require more accurate quantification of drug loading and release profiles through the
13 use of assays such as HPLC analysis and *in-vitro/in-vivo* models. However, these results verify
14 transdermal delivery of the model drug from reservoir-tipped needles. Delivery trends are as expected,
15 and show that this novel needle design offers a promising method of transdermal delivery.
16
17
18
19
20
21

22 **3.4 Reliability**

23
24 During post-insertion inspection, it was noted that a significant number of needles suffered minor tip
25 damage during the skin delivery tests. One array was damaged after removal due to manual handling,
26 and, of the other five arrays that completed a full inspection, 33% of all needles indicated some degree
27 of tip damage. This was always confined to the tip region and no major structural failures of the body
28 of the microneedles were observed. Needle tips seemed to be flattened or crushed, i.e. no breakage or
29 brittle fracture was seen. It is therefore unlikely that any material remained in the skin after use, and,
30 as these are single-use devices, this tip blunting should not pose a major issue. It is nevertheless
31 undesirable and other polymers and/or tip designs should be investigated.
32
33
34
35
36
37

38 **4 Conclusion**

39
40 This paper has shown that two low-cost techniques – injection moulding and inkjet printing – may be
41 combined to produce coated microneedles for transdermal drug and vaccine delivery. Initially, μ SL
42 was used to produce 475 μ m tall microneedles, which featured a flat-bottomed pit or reservoir located
43 close to the needle tip. This reservoir increases loading capacity and removes the need to tilt samples
44 in order to present a flat surface to the incoming droplet.
45
46
47
48

49 These designs were then replicated at a commercial injection-moulding facility, using a modified
50 process based on former CD/DVD production equipment. An inkjet printer was used to deposit a
51 model drug (FITC) into the reservoir, and needle arrays were inserted into *ex-vivo* human skin using
52 an applicator. Subsequent fluorescence analysis showed the results were largely in line with
53 expectations, i.e. intensity increased with needle loading and skin insertion time. This work shows
54 that it is feasible to rapidly produce large quantities of coated microneedle arrays, using automated
55 processes, in medical-grade material and at low cost.
56
57
58
59
60

Acknowledgement

This work was financially supported by the BMVIT - Bundesministerium für Verkehr, Innovation und Technologie (Austria) and was conducted in the framework of the program "Production of the future" (MicroNeedle, Grant 853482). This work has also been partially supported by the Science Foundation Ireland INSIGHT Centre, by Enterprise Ireland (CF/2012/2339), and by the Higher Education Authority under the Programme for Research in Third-Level Institutions.

References

- [1] A. C. Watkinson, "A commentary on transdermal drug delivery systems in clinical trials," *Journal of Pharmaceutical Sciences* **102**, pp. 3082-3088, 2013.
- [2] M. R. Prausnitz and R. Langer, "Transdermal drug delivery," *Nature biotechnology* **26**, pp. 1261-8, 2008.
- [3] A. Morteza, S. Sahar, N. B. J., and S. Metin, "Recent Advances in Wearable Transdermal Delivery Systems," *Advanced Materials* **30**, p. 1704530, 2018.
- [4] C. M. Niessen, "Tight junctions/adherens junctions: basic structure and function," *Journal of Investigative Dermatology* **127**, pp. 2525-2532, 2007.
- [5] M. R. Prausnitz, "Engineering microneedle patches for vaccination and drug delivery to skin," *Annual review of chemical and biomolecular engineering* **8**, pp. 177-200, 2017.
- [6] K. Ita, "Transdermal Delivery of Drugs with Microneedles—Potential and Challenges," *Pharmaceutics* **7**, p. 90, 2015.
- [7] J. B. Carey, F. E. Pearson, A. Vrdoljak, M. G. McGrath, A. M. Crean, P. T. Walsh, *et al.*, "Microneedle array design determines the induction of protective memory CD8+ T cell responses induced by a recombinant live malaria vaccine in mice," *PLoS One* **6**, p. e22442, 2011.
- [8] M. Dul, M. Stefanidou, P. Porta, J. Serve, C. O'Mahony, B. Malissen, *et al.*, "Hydrodynamic gene delivery in human skin using a hollow microneedle device," *Journal of Controlled Release* **265**, pp. 120-131, 2017.
- [9] R. Haj-Ahmad, H. Khan, M. S. Arshad, M. Rasekh, A. Hussain, S. Walsh, *et al.*, "Microneedle Coating Techniques for Transdermal Drug Delivery," *Pharmaceutics* **7**, pp. 486-502, 2015.
- [10] M. Leone, J. Mönkäre, J. A. Bouwstra, and G. Kersten, "Dissolving Microneedle Patches for Dermal Vaccination," *Pharmaceutical research* **34**, pp. 2223-2240, 2017.
- [11] S. Henry, D. V. McAllister, M. G. Allen, and M. R. Prausnitz, "Microfabricated microneedles: a novel approach to transdermal drug delivery," *Journal of pharmaceutical sciences* **87**, pp. 922-925, 1998.
- [12] C. O'Mahony, "Structural characterization and in-vivo reliability evaluation of silicon microneedles," *Biomedical microdevices* **16**, pp. 333-343, 2014.
- [13] S. Indermun, R. Luttge, Y. E. Choonara, P. Kumar, L. C. Du Toit, G. Modi, *et al.*, "Current advances in the fabrication of microneedles for transdermal delivery," *Journal of controlled release* **185**, pp. 130-138, 2014.
- [14] C. O'Mahony, K. Grygoryev, A. Ciarlone, G. Giannoni, A. Kenthao, and P. Galvin, "Design, fabrication and skin-electrode contact analysis of polymer microneedle-

- 1
2
3 based ECG electrodes," *Journal of Micromechanics and Microengineering* **26**, p.
4 084005, 2016.
- 5
6 [15] E. A. Allen, C. O'Mahony, M. Cronin, T. O'Mahony, A. C. Moore, and A. M. Crean,
7 "Dissolvable microneedle fabrication using piezoelectric dispensing technology,"
8 *International journal of pharmaceutics* **500**, pp. 1-10, 2016.
- 9
10 [16] X. Hong, L. Wei, F. Wu, Z. Wu, L. Chen, Z. Liu, *et al.*, "Dissolving and biodegradable
11 microneedle technologies for transdermal sustained delivery of drug and vaccine,"
12 *Drug design, development and therapy* **7**, p. 945, 2013.
- 13
14 [17] K. Ita, "Dissolving microneedles for transdermal drug delivery: Advances and
15 challenges," *Biomedicine & Pharmacotherapy* **93**, pp. 1116-1127, 2017.
- 16
17 [18] J. D. Kim, M. Kim, H. Yang, K. Lee, and H. Jung, "Droplet-born air blowing: novel
18 dissolving microneedle fabrication," *Journal of controlled release* **170**, pp. 430-436,
19 2013.
- 20
21 [19] K. Lee and H. Jung, "Drawing lithography for microneedles: a review of fundamentals
22 and biomedical applications," *Biomaterials* **33**, pp. 7309-7326, 2012.
- 23
24 [20] L. Zema, G. Loreti, A. Melocchi, A. Maroni, and A. Gazzaniga, "Injection Molding and
25 its application to drug delivery," *Journal of Controlled Release* **159**, pp. 324-331,
26 2012.
- 27
28 [21] U. M. Attia, S. Marson, and J. R. Alcock, "Micro-injection moulding of polymer
29 microfluidic devices," *Microfluidics and Nanofluidics* **7**, p. 1, 2009.
- 30
31 [22] D. Duan, C. Moeckly, J. Gysbers, C. Novak, G. Prochnow, K. Siebenaler, *et al.*,
32 "Enhanced delivery of topically-applied formulations following skin pre-treatment
33 with a hand-applied, plastic microneedle array," *Current drug delivery* **8**, pp. 557-65,
34 2011.
- 35
36 [23] S. Kommareddy, B. C. Baudner, A. Bonificio, S. Gallorini, G. Palladino, A. S. Determan,
37 *et al.*, "Influenza subunit vaccine coated microneedle patches elicit comparable
38 immune responses to intramuscular injection in guinea pigs," *Vaccine* **31**, pp. 3435-
39 41, 2013.
- 40
41 [24] Y. Zhang, K. Brown, K. Siebenaler, A. Determan, D. Dohmeier, and K. Hansen,
42 "Development of Lidocaine-Coated Microneedle Product for Rapid, Safe, and
43 Prolonged Local Analgesic Action," *Pharmaceutical research* **29**, pp. 170-177, 2012.
- 44
45 [25] S. A. Burton, C.-Y. Ng, R. Simmers, C. Moeckly, D. Brandwein, T. Gilbert, *et al.*, "Rapid
46 intradermal delivery of liquid formulations using a hollow microstructured array,"
47 *Pharmaceutical research* **28**, pp. 31-40, 2011.
- 48
49 [26] K. B. Mirza, C. Zuliani, B. Hou, F. S. Ng, N. S. Peters, and C. Toumazou, "Injection
50 moulded microneedle sensor for real-time wireless pH monitoring," in *2017 39th
51 Annual International Conference of the IEEE Engineering in Medicine and Biology
52 Society (EMBC)*, 2017, pp. 189-192.
- 53
54 [27] K. Nair, B. Whiteside, C. Grant, R. Patel, C. Tuinea-Bobe, K. Norris, *et al.*,
55 "Investigation of Plasma Treatment on Micro-Injection Moulded Microneedle for
56 Drug Delivery," *Pharmaceutics* **7**, pp. 471-85, 2015.
- 57
58 [28] F. Sammoura, J. Kang, Y.-M. Heo, T. Jung, and L. Lin, "Polymeric microneedle
59 fabrication using a microinjection molding technique," *Microsystem Technologies* **13**,
60 pp. 517-522, 2007.
- [29] K. Yung, Y. Xu, C. Kang, H. Liu, K. Tam, S. Ko, *et al.*, "Sharp tipped plastic hollow
microneedle array by microinjection moulding," *Journal of Micromechanics and
microengineering* **22**, p. 015016, 2011.

- 1
2
3
4 [30] S. H. Lim, H. Kathuria, J. J. Y. Tan, and L. Kang, "3D printed drug delivery and testing
5 systems — a passing fad or the future?," *Advanced Drug Delivery Reviews* 2018.
- 6 [31] A. Aksit, D. N. Arteaga, M. Arriaga, X. Wang, H. Watanabe, K. E. Kasza, *et al.*, "In-vitro
7 perforation of the round window membrane via direct 3-D printed microneedles,"
8 *Biomedical Microdevices* **20**, p. 47, 2018.
- 9 [32] K. Mincho, P. Jose Efrain, I. Yurii, B. Andrea, L. Carlo, and K. Jürgen, "Biocompatible
10 3D printed magnetic micro needles," *Biomedical Physics & Engineering Express* **3**, p.
11 025005, 2017.
- 12 [33] Y. Lu, S. N. Mantha, D. C. Crowder, S. Chinchilla, K. N. Shah, Y. H. Yun, *et al.*,
13 "Microstereolithography and characterization of poly (propylene fumarate)-based
14 drug-loaded microneedle arrays," *Biofabrication* **7**, p. 045001, 2015.
- 15 [34] S. H. Lim, J. Y. Ng, and L. Kang, "Three-dimensional printing of a microneedle array on
16 personalized curved surfaces for dual-pronged treatment of trigger finger,"
17 *Biofabrication* **9**, p. 015010, 2017.
- 18 [35] C. O'Mahony, L. Hilliard, T. Kosch, A. Bocchino, E. Sulas, A. Kenthao, *et al.*, "Accuracy
19 and feasibility of piezoelectric inkjet coating technology for applications in
20 microneedle-based transdermal delivery," *Microelectronic Engineering* **172**, pp. 19-
21 25, 2017.
- 22 [36] M. J. Uddin, N. Scoutaris, P. Klepetsanis, B. Chowdhry, M. R. Prausnitz, and D.
23 Douroumis, "Inkjet printing of transdermal microneedles for the delivery of
24 anticancer agents," *International Journal of Pharmaceutics* **494**, pp. 593-602, 2015.
- 25 [37] R. D. Boehm, P. R. Miller, S. L. Hayes, N. A. Monteiro-Riviere, and R. J. Narayan,
26 "Modification of microneedles using inkjet printing," *AIP Advances* **1**, p. 022139,
27 2011.
- 28 [38] R. D. Boehm, P. R. Miller, W. A. Schell, J. R. Perfect, and R. J. Narayan, "Inkjet Printing
29 of Amphotericin B onto Biodegradable Microneedles Using Piezoelectric Inkjet
30 Printing," *JOM* **65**, pp. 525-533, 2013.
- 31 [39] R. D. Boehm, P. R. Miller, J. Daniels, S. Stafslie, and R. J. Narayan, "Inkjet printing for
32 pharmaceutical applications," *Materials Today* **17**, pp. 247-252, 2014.
- 33 [40] R. D. Boehm, J. Daniels, S. Stafslie, A. Nasir, J. Lefebvre, and R. J. Narayan,
34 "Polyglycolic acid microneedles modified with inkjet-deposited antifungal coatings,"
35 *Biointerphases* **10**, p. 011004, 2015.
- 36 [41] R. D. Boehm, P. Jaipan, S. A. Skoog, S. Stafslie, L. VanderWal, and R. J. Narayan,
37 "Inkjet deposition of itraconazole onto poly (glycolic acid) microneedle arrays,"
38 *Biointerphases* **11**, p. 011008, 2016.
- 39 [42] C. P. P. Pere, S. N. Economidou, G. Lall, C. Ziraud, J. S. Boateng, B. D. Alexander, *et al.*,
40 "3D printed microneedles for insulin skin delivery," *International Journal of*
41 *Pharmaceutics* **544**, pp. 425-432, 2018.
- 42 [43] K. Schossleitner, C. O'Mahony, S. Brandstatter, M. J. Haslinger, S. Demuth, D. Fechtig,
43 *et al.*, "Differences in biocompatibility of microneedles from cyclic olefin polymers
44 with human endothelial and epithelial skin cells," *Journal of biomedical materials*
45 *research. Part A* **107**, pp. 505-512, 2019.
- 46 [44] (2019, 15 April). *SD40E Disc Molding Subsystem*. Available: [http://www.sumitomo-](http://www.sumitomo-shi-demag.us/sd40emain.html)
47 [shi-demag.us/sd40emain.html](http://www.sumitomo-shi-demag.us/sd40emain.html)
- 48 [45] T. RR Singh, N. J Dunne, E. Cunningham, and R. F Donnelly, "Review of patents on
49 microneedle applicators," *Recent Patents on Drug Delivery & Formulation* **5**, pp. 11-
50 23, 2011.
- 51
52
53
54
55
56
57
58
59
60

- 1
2
3 [46] G. Li, A. Badkar, S. Nema, C. S. Kolli, and A. K. Banga, "In vitro transdermal delivery of
4 therapeutic antibodies using maltose microneedles," *International journal of*
5 *pharmaceutics* **368**, pp. 109-115, 2009.
6
7 [47] C. T. Rueden, J. Schindelin, M. C. Hiner, B. E. DeZonia, A. E. Walter, E. T. Arena, *et al.*,
8 "ImageJ2: ImageJ for the next generation of scientific image data," *BMC*
9 *Bioinformatics* **18**, p. 529, 2017.
10
11
12
13
14
15
16
17
18
19
20
21
22
23
24
25
26
27
28
29
30
31
32
33
34
35
36
37
38
39
40
41
42
43
44
45
46
47
48
49
50
51
52
53
54
55
56
57
58
59
60

Accepted Manuscript